GDCh Research Article Angewandte International Edition Chemie www.angewandte.org

How to cite: *Angew. Chem. Int. Ed.* **2025**, *64*, e202417179
doi.org/10.1002/anie.202417179

Synthetic Methods

Selective Deuteration and Tritiation of Pharmaceutically Relevant Sulfoximines

*Blair I. P. Smith, Nathan M. L. Knight, Gary J. Knox, David M. Lindsay, Laura C. Paterson, Jonas Bergare, Charles S. Elmore, Ryan A. Bragg, and William J. Kerr**

Abstract: Pharmaceutical-aligned research endeavors continue to diversify, including via the installation of new chemical functionality and non-classical bioisosteres within drug design. With this, an equally high demand emerges for the direct installation of isotopic substituents into these scaffolds within drug discovery programmes, as isotopologues are essential for the elucidation of the biological efficacy and metabolic fate of the active pharmaceutical ingredient (API). The sulfoximine functional group has recently become established as a high-value unit in this context; however, general and effective methods for the synthesis of deuterium (^{2}H, D) and tritium (^{3}H, T) labelled analogues have remained elusive. Herein, we disclose the design and development of the first iridium-catalyzed sulfoximine-directed hydrogen isotope exchange (HIE) systems that permit the site-selective integration of a distinguishing atomic label at aromatic C(sp^2)–H and more challenging C(sp^3)–H moieties. Moreover, we exemplify the broad applicability of these methods within a spectrum of molecular settings, as well as in the late-stage generation of isotopically-enriched complex bioactive architectures.

[*] B. I. P. Smith, Dr. N. M. L. Knight, Dr. G. J. Knox, Dr. D. M. Lindsay, Dr. L. C. Paterson, Prof. Dr. W. J. Kerr
Department of Pure and Applied Chemistry
University of Strathclyde
295 Cathedral Street, Glasgow, Scotland, G1 1XL (UK)
E-mail: w.kerr@strath.ac.uk
Homepage: https://williamjkerr.com

J. Bergare, Dr. C. S. Elmore
Early Chemical Development
Pharmaceutical Sciences, R&D, AstraZeneca, Gothenburg, SE-43183 (Sweden)

Dr. R. A. Bragg
Early Chemical Development
Pharmaceutical Sciences, R&D, AstraZeneca, Cambridge, England, CB2 0AA (UK)

Introduction

Modern medicinal chemistry has focused heavily on creating new molecular structures to find solutions for important biological targets that have been challenging to address.[1] With the pharmaceutical properties of bioactive molecules intimately related to the functionality embedded within their structural architectures, strategic leveraging of the redox states of the sulfur atom has been employed to access numerous functional groups that allow the modulation of the biological activity of drug candidates with minimal adverse impact on the physicochemical profile.[2] More specifically, sulfur(VI) groups are frequently employed as pharmacophores within drug discovery campaigns and are highly represented in this domain; more specifically, greater than 90 therapeutics approved by the US Food and Drug Administration (FDA) overall,[3] and 32 % of small-molecule drugs approved in 2022, possess this compound class.[4]

Among these motifs, sulfoximines, mono-aza analogues of sulfones, have gathered heightened importance (Figure 1A).[5] The utility of such sulfoximine-containing structures derives from their diverse structural potential and versatile nature, as the additional vector the nitrogen atom provides can enable exploration of unmapped chemical space. Additionally, the stereocontrolled synthesis of sulfoximine fragments can deliver configurationally and conformationally stable compounds, whilst also benefiting from unique additional properties such as hydrogen-bond donor/acceptor modes, high metabolic stability, and favorable solubility in protic solvents (Figure 1B).[6] With these properties brought recently to light, the pharmaceutical value of such structures has been realised for the enhancement of physicochemical and pharmacokinetic properties of drug molecules.[7]

To support the progress of emerging drug candidates, an understanding of their biological fate is of fundamental importance.[8] Associated with this, deuterium- and tritium-labelled compounds have become invaluable tools for in vitro and in vivo studies, due to these isotopologues closely reflecting the biological activity of the parent C–H containing analogue.[9] Therefore, the installation of such an isotopic unit provides a distinguishing label that can be exploited for the direct tracing and quantification of a compound's metabolic profile. In addition to this, more recently, the isosteric replacement of protium for deuterium has been extensively investigated for the fine-tuning of the pharmaceutical properties of drug candidates

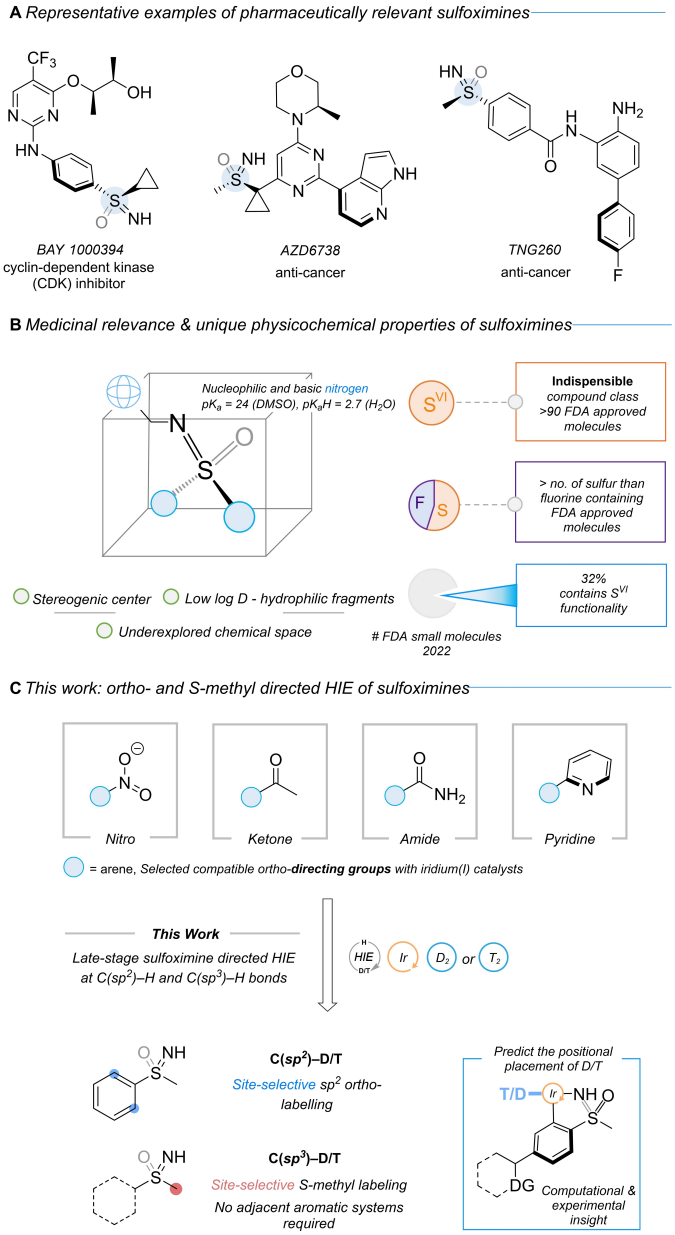

Figure 1. **A** Representative examples of pharmaceutically relevant sulfoximines. **B** Medicinal relevance & unique physicochemical properties of sulfoximines. **C** This work: *ortho*- and *S*-methyl directed HIE of sulfoximines.

themselves.[10] In any case, drug molecules highly enriched with deuterium are employed in toxicological, metabolism, and pharmacokinetic studies, where they are employed as internal standards for quantitative mass spectrometry-based analysis (LC–MS/MS).[11] This enables the timely evaluation of promising candidates, in attempts to combat the high attrition rates associated with early drug development.[12] With regards tritium, molecules with high-specific activity are vital research tools in the in vivo visualisation of drugs, as well as in nanomolar receptor-ligand binding assays.[9,13]

Aligned with such applications as those described above, transition metal-catalyzed hydrogen isotope exchange (HIE) has emerged as a leading technology for the preparation of deuterium- or tritium-containing organic molecules.[14] In particular, iridium-catalyzed HIE methodologies have enabled isotopic incorporation at aromatic and heteroaromatic C(sp^2)–H sites located *ortho* to a suitable directing group (DG), with deuterium (D_2) and tritium gas (T_2) employed as the sole isotopic source.[15] Within this field, a suite of iridium(I) carbene complexes has been developed in our laboratories, which are tailored towards the rapid late-stage generation of selectively labelled compounds, and facilitated by an extensive array of directing groups (Scheme 1C).[16–19] Other state-of-the-art methods include those devised by the Chirik[20] and MacMillan[21] groups, which provide orthogonal and complementary strategies. The former introduces tritium at the most sterically accessible C(sp^2)–H bond, meanwhile the latter facilitates exchange with high site selectivity adjacent to tertiary amine units. Work from our own group has aimed to establish methods that can satisfy the broadest applicability, mainly through programming our iridium catalyst range to engage with emerging pharmaceutically-relevant functionality as directing groups, whilst also expanding our functionalization strategies beyond the C(sp^2)–H *ortho*-position to provide a highly enabling catalytic platform for HIE. Related to this, our systems have recently been expanded to deliver directed labelling into more challenging C(sp^3)–H bonds,[22] and we have also reported the first direct catalytic method for formyl-selective deuterium labeling on aromatic aldehydes.[23] Aligned with all of this, within pharmaceutical studies, the site of the label can be of appreciable importance, with the susceptibility of the C(sp^2/sp^3)–D/T moieties themselves to undergo protium exchange under physiological conditions being a further key consideration.[8d] Indeed, for application within de novo deuterated drug design, HIE methods must be both site-selective and capable of delivering robust and reliably labelled products.[10]

Based on all of this, we envisioned that the iridium(I) catalyst methods established within our laboratory could be further expanded, through a synergistic experimentally- and computationally-guided approach, to deliver previously unprecedented HIE methods for application with a collection of pharmaceutically-relevant sulfoximine architectures. In line with our previous studies, we sought to develop an *ortho*-directed labelling strategy mediated via the sulfoximine functional group. Extending from this, we postulated that through computational analysis of the catalytic cycle, we could develop a method for the straightforward prediction of the regioselectivity of the HIE process within densely functionalized complex molecules, thus serving to accelerate the synthesis of both deuterated and tritiated materials. Moreover, as part of this overarching study we also uncovered a novel C–H activation pathway at more challenging to label C(sp^3)–H centers located at the *S*-methyl position of the sulfoximine unit. Collectively, we report catalytic labelling protocols which offer one convenient synthetic method to forge

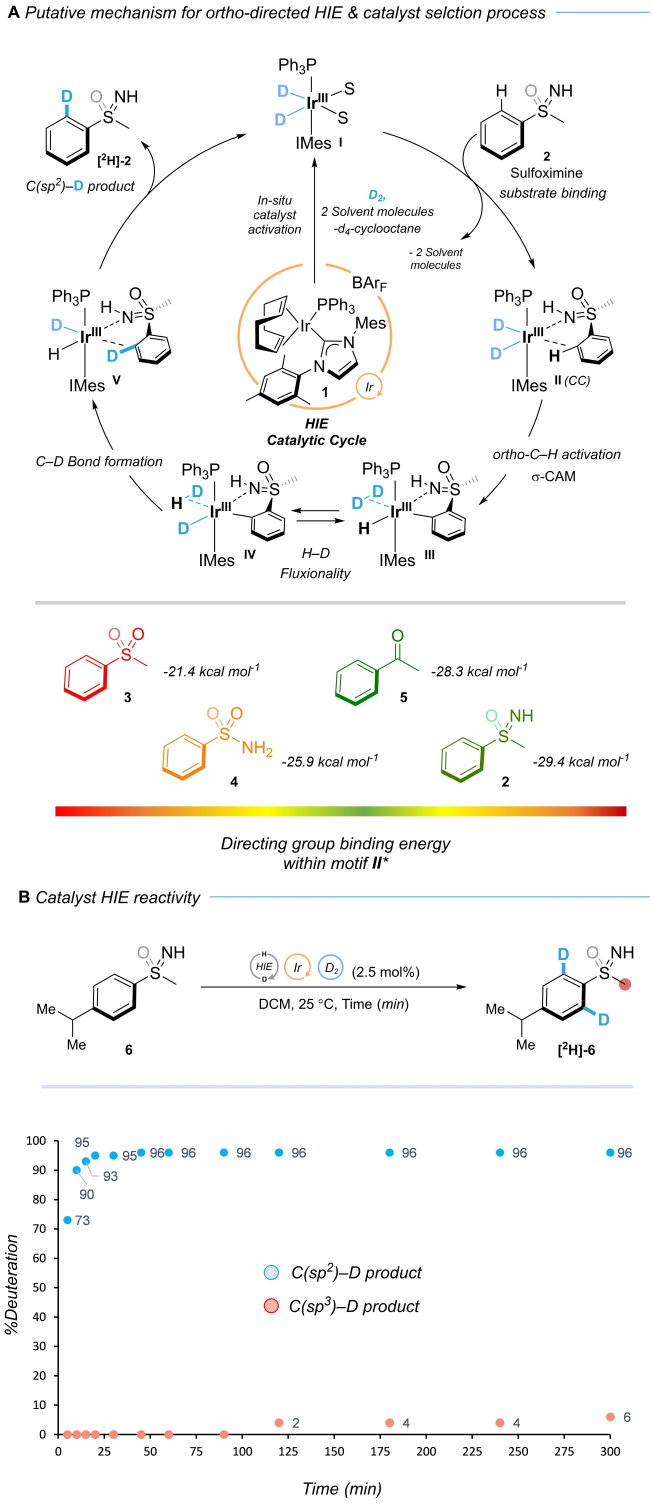

Scheme 1. Pre-catalyst selection and optimization process. **A** Putative mechanism for *ortho*-directed HIE & catalyst selection process. Binding energies calculated at the 6-311G(d,p) level of theory. *Protium equivalents used in these calculations. **B** Catalyst HIE reactivity.

C–D and C–T bonds within both C(sp^2)- and C(sp^3)-rich sulfoximine-containing compounds for the first time (Figure 1C).

Results and Discussion

To begin, our studies focused on the commercially available, and air- and moisture-stable, [Ir(COD)(PPh_3)-(IMes)]BAr_F complex **1** for mechanistic and computational analysis concerned with the desired *ortho*-directed C–H functionalization reaction. We envisioned that the core catalytic cycle shown in Scheme 1A, as previously formulated in our laboratories,[16b] and building on a mechanism previously proposed by Heys,[24] could be applicable to sulfoximine substrates. The cycle starts with in situ activation of pre-catalyst **1** with D_2 gas, driving extrusion of d_4-cyclooctane and affording the bis-solvated active catalyst **I**. From here, complexation of the nitrogen atom within sulfoximine **2**, and engagement with the *ortho*-C(sp^2)–H site via formation of an agostic interaction, would generate the coordination complex (CC) **II**. This substrate bound species could subsequently undergo site-selective C–H activation through a σ-complex assisted metathesis (σ-CAM) process[25] to provide the 5-membered metallocyclic intermediate (5-mmi) species **III**. Following this, hydride fluxionality would deliver the deuterium atom *cis* to the σ-aryl ligand, from which a reverse dual redox process could ensue, allowing liberation of the desired functionalized C(sp^2)–D neutron-enriched product **[²H]-2**, with substrate turn-over regenerating iridium complex **I**.

Considering this mechanistic sequence, based on precedent from our laboratory, we anticipated that the substrate binding event could be central to a successful HIE process. More specifically, having considered the required balance between co-ordination and dissociation events for productive catalysis, we have previously utilized substrate binding energy as a guiding principle for both catalyst and associated reaction system design, alongside the provision of mechanistic insight.[16b,f,17,18a,26,27] Therefore, as a prelude to experimentally exploring the reactivity of the sulfoximine unit, we employed the computationally-derived binding energy[28] to assess the affinity between the substrate and iridium(III) catalyst within the coordination complex motif present in intermediate **II**. Accordingly, we calculated and compared the binding energy of the readily labelled acetophenone **5** to that of sulfur(VI) directing groups, as shown in Scheme 1A. In stark contrast to the ketone-directing substrate **5**, the sulfur-based compounds sulfone **3** and sulfonamide **4** possess a tetrahedral molecular geometry and distinct chemical compositions that inevitably lead to lower and insufficient binding energies to allow for productive labelling within this system[26,27] (−21.4 and −25.9 kcal mol^{-1}, respectively, as compared with −28.3 kcal mol^{-1} for acetophenone). Indeed, with regards our sulfone- and sulfonamide-directed HIE approaches, it is necessary to adopt more accessible iridium-based coordination spheres.[26,27] In contrast to these sulfur-directing groups, theoretical analysis suggested a more favorable binding energy value of −29.4 kcal mol^{-1} for sulfoximine substrate **2**. To further support this potentially positive prediction of HIE capability, additional density functional theory (DFT) calcu-

lations revealed that the transition state for C–H activation, interconnecting intermediates **II** and **III**, was seemingly facile for sulfoximine **2** at 22.5 kcal mol^{-1} (see the Supporting Information for the fully calculated potential energy surface (PES)). It should also be noted that further computational analysis was carried out to evaluate the binding energies of sulfoximine **2** with varying iridium catalyst types from our laboratories, with complex **1** remaining optimal (see the Supporting Information for full details).

Encouraged by our theoretical insights, the deuteration of sulfoximine **6** using iridium(I) (PPh_3/IMes) pre-catalyst **1** was selected as our prototypical system (Scheme 1B). Our initial experiment involved a time study, with a reaction system composed of 2.5 mol % metal-complex loading and an atmosphere of D_2 delivered by balloon at 25 °C in DCM. Pleasingly, an isotopic labelling level of 73 % was delivered in only 5 minutes and, with further extension of the reaction time to 20 minutes and beyond, a plateau at 96 % incorporation was observed. Notably, our study underscored the importance of reaction time, as at around the 2 hour point the *S*-methyl position also engaged in the less reactive C-(sp^3)–H activation and exchange, albeit to only a minimal degree. From the collected data, we envisioned that a 1 hour reaction time had the potential to provide a regioselective procedure for the incorporation of deuterium at the *ortho*-C(sp^2)–H positions.

Based on the initial outputs with our pre-catalyst **1**, a solvent scope study was conducted, which confirmed a strong performance of our developing HIE protocol across a spectrum of reaction media (Scheme 2). More specifically, model substrate **6** was applied with excellent levels of C(sp^2)–H incorporation (≥82 % D) obtained across 11 solvents. Accompanying deuteration of 5 % D and 6 % D at the *S*-methyl position was also witnessed with solvents IPA and 2-MeTHF, respectively. This broad solvent applicability highlights the potential compatibility of this method with emerging sulfoximine derivatives possessing a range of solubility profiles.

Next, we evaluated the generality of the labelling process with a range of N–H containing sulfoximines. Pleasingly, parent sulfoximine **2** was readily deuterated to deliver **[^{2}H]-2** (93 % D). Using the same substrate, and taking advantage of how solvent affects labelling at the *S*-methyl position, the reaction conditions were adjusted by elevating catalyst loading, reaction time, and temperature in 2-MeTHF to enable the synthesis of a highly deuterated analogue of **2** (C(sp^2)–H 93 % D and C(sp^3)–H 77 % D). Following this, under the standard mild original conditions, we accomplished modular access to all *ortho*-deuterated methyl-substituted permutations of the arene ring (**[^{2}H]-7**–**9**, 78–96 % D), with a greater bias for the sterically unhindered site within **[^{2}H]-8** being observed. Arenes bearing useful synthetic features, **10** and **11**, or a key pharmacophore, **12**, were readily applicable within this transformation (**[^{2}H]-10**; 96 % D; **[^{2}H]-11**, 87 % D; and **[^{2}H]-12**, 95 % D, respectively), with the former compounds primed for downstream manipulation. Moreover, electron-rich aromatic rings proved to be excellent substrates, with high degrees of deuterium exchange achieved within products **[^{2}H]-13** and **[^{2}H]-14**, the latter performing most efficiently using EtOH as the reaction medium. Notably, when the *para*-substituted substrate **14** was subjected to an extended reaction time of 4 hours, the ethanol solvent appears to function as a protium source to fuel the backward exchange process, in turn, limiting access to the desired deuterated product (**[^{2}H]-14**, 90 % D in 1 h, versus 78 % D in 4 h); also see the Supporting Information for additional insight. Substrate **15**, containing a sterically demanding *ortho*-bromo functionality, proceeded smoothly (94 % D), and the unhindered position in **16** was exclusively labelled (91 % D). In contrast to this, **17** was found to label across both steric environments (96 % D at both *ortho*-positions). The 2-naphthyl sulfoximine, **18**, also saw good levels of incorporation at the two *ortho*-sites, whereas the diphenyl system led to excellent 95 % labelling over the four available *ortho*-positions (**[^{2}H]-19**). Next, we investigated the relationship between structural derivatisation of the *S*-methyl position and the performance of our labelling system (**19**–**23**). In relation to this, we were particularly pleased to uncover that the substrate appended with an *iso*-propyl group proximal to the directing group proceeded efficiently (**[^{2}H]-20**, 97 % D), however, systematic addition of a further methyl group, with *tert*-butyl derivative **21**, did lower the isotopic incorporation to 68 % D. Deuterium was also successfully installed within systems possessing a cyclopropyl *S*-substituent and a fused-bicyclic scaffold (**[^{2}H]-22** and **[^{2}H]-23**, 95 % D and 98 % D, respectively). Finally as related to N–H sulfoximines, incorporation was also efficiently realised within the furan heteroarene system (**[^{2}H]-24**, 97 %).

As shown in Scheme 2, the developed catalytic method was also fully translatable to sulfonimidamides, with regioselective enrichment maintained in the presence of adjacent pharmacophoric saturated heterocycles, morpholine (**[^{2}H]-25**, 95 % D) and piperazine (**[^{2}H]-26**, 96 % D). Following this, we extended our protocol to applications with *N*-functionalized sulfoximines, as this handle presents the opportunity for the fine-tuning of pharmacokinetic and physiochemical properties within emerging drug units. Accordingly, a small-library of *N*-functionalized sulfoximines were labelled (**27**–**35**), with *N*-ethylated and saturated heterocyclic cores compatible under standard conditions (**[^{2}H]-27** and **[^{2}H]-28**, 90 % D and 97 % D, respectively). Further substitution within the *N*-group inhibited the process in some cases; however, catalytic activity could be reinstated through reducing steric hindrance around the ligand coordination sphere. More specifically, reducing the percent buried volume (%V_{bur})[29] of the iridium complex through rational replacement of the auxiliary PPh_3 ligand with PMe_2Ph (28.1 versus 23.2 %V_{bur} within intermediate **II**, respectively) afforded product **[^{2}H]-29** with 96 % *ortho*-deuteration, alongside minimal *S*-methyl labelling. With regards competing functionalization, dependent on the catalyst and reaction conditions, varying levels of C(sp^2) and C(sp^3)

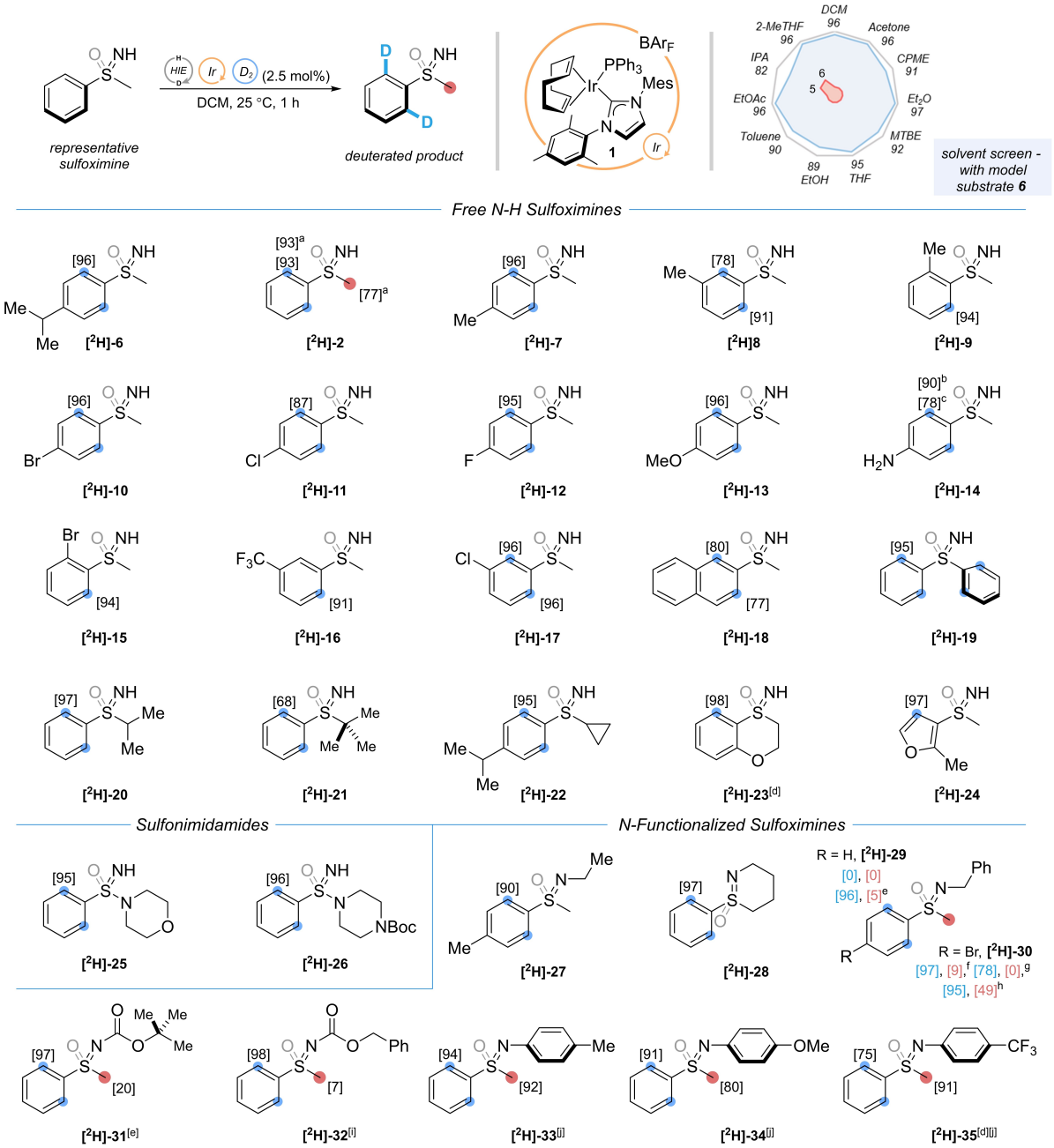

Scheme 2. Evaluation of the scope associated with the *ortho*-directed C–H activation sequence. All reactions were performed on a 0.1075 mmol scale with 2.5 mol% of pre-catalyst **1** under an atmosphere of deuterium introduced via balloon, and in DCM (0.043 M) at 25 °C over 1 h; isotopic incorporation within the isolated products is recorded as an average of, at least, two separate runs. [a]Reaction conducted with 5 mol% of pre-catalyst **1** in 2-MeTHF at 50 °C over 16 h. [b]Ethanol was used as the solvent. [c]Ethanol used as the solvent over a reaction time of 4 hours. [d]Incorporation was determined from the crude reaction mixture. [e][Ir(COD)(PMe$_2$Ph)(IMes)]BAr$_F$ complex **36** (2.5 mol%) was employed at 30 °C. [f]Reaction performed at 30 °C over 30 minutes. [g]Reaction performed at 30 °C using 1 mol% of pre-catalyst **1**. [h][Ir(COD)(PMe$_2$Ph)(IMes)]BAr$_F$ **36** (2.5 mol%) was employed at 30 °C over 4 hours. [i][Ir(COD)(PMe$_2$Ph)(IMes)]BAr$_F$ complex **36** (2.5 mol%) was employed. [j]Reaction time was extended to 4 hours.

labelling were achieved with substrate **30**, with control of (C(sp^2)–H) selectivity possible when lowered levels of catalyst **1** were employed.

Even further elaborated sulfoximine structures **31**–**35** were proficient under the developed catalyst system, with generally excellent C(sp^2)–H labelling levels achievable with either parent PPh_3 catalyst, **1**, or the PMe_2Ph complex, **36**. As detailed in Scheme 2, even electronically diverse *N*-arylated sulfoximines **33**–**35** proved to be effective substrates, with both C(sp^2)–H and C(sp^3)–H sites undergoing H/D exchange in concomitant fashion. A regioselective process could not be achieved with these three latter substrates; nonetheless, such highly deuterated derivatives are often desired as suitably labelled

substrates within the early stage ADME domain.[9,11] To further understand these *N*-arylated substrates, the rates for the respective labelling pathways (C(sp^2) versus C-(sp^3)) were measured and found to be highly competitive at $4.99\times10^{-4}\,s^{-1}$ and $4.24\times10^{-4}\,s^{-1}$, respectively, for the reaction of **33**, explaining the challenge faced here with regards labelling selectivity (see the Supporting Information for full details).

When considering polyfunctionalized substrates, the ability to successfully predict the positional placement of isotopic substituents within such complex molecules has the potential to expedite the synthesis of selectively enriched materials. Related to this, a recent report from Derdau and co-workers[30] outlined a general directing group scale using DFT calculations that identified the iridium-substrate coordination complex (CC; cf. **II** in Scheme 1A) as the species primarily responsible for the regiochemical outcome of a HIE reaction. This approach delivered accurate predictions for simple substrates and was then extended to a number of more complex pharmaceutical examples. However, the theoretical insight from this earlier study was linked directly to the monosubstituted arenes from which the directing group scale was constructed. We thus looked to build on this work through consideration of the binding energies associated with the possible CCs within specific polyfunctionalized molecules. It was envisaged that application of this more direct approach would, consequently, result in more accurate predictions, accounting for both the location of the coordinating groups and the innate electronics of the arene to be labelled.

As such, we conducted intramolecular competition reactions on a series of bifunctional sulfoximine containing molecules (**37**–**40**), under standard conditions, alongside computing the optimized geometries of their respective CCs in silico (Scheme 3A). The competing directing groups are arranged by increasing calculated binding energy left to right. Experimentally, the sulfoximine moiety facilitated excellent levels of labelling regioselectivity for this reaction type, when considering a non-heteroaromatic competing directing group, with exclusive incorporation witnessed in the face of nitro **37**, ester **38**, and ketone **39** functional handles. Importantly, the derived binding energies strongly aligned with the experimental outcomes, with the sulfoximine moiety's greater affinity for the cationic metal-center dominating the outcome of the arene functionalization process. In contrast, the planar pyridine group was revealed to be the stronger directing unit; nonetheless, a notable 28 % D enrichment was also observed *ortho* to the sulfoximine. Further calculations confirmed that no correlation exists between other salient steps within the catalytic cycle and the relative positional enrichment (see the Supporting Information for further details).

To highlight the translatability and late-stage functionalization potential of our *ortho*-directed C–H exchange protocol to structures of more elevated levels of complexity, we targeted the direct labelling of pharmaceutically relevant scaffolds. Accordingly, we targeted deuterated and tritiated analogues of the cancer drug BAY1000394 (Roniciclib) **42**[7c,31] as the structural configuration of the functional groups within this molecule present a potentially competitive environment for HIE, thus providing an opportunity for regiochemical outcome prediction. As outlined in Schemes 3B and 3C, the aromatic ring embedded within the core of the molecule can undergo C–H activation through the sulfoximine or pyrimidine groups, via a 5-mmi or, normally more energy intensive,[16b] 6-mmi pathway, respectively. Thus, we endeavored to fully compute the anticipated intermediates along the reaction coordinate for both directing functionalities and compared the associated energies of each to allow a prediction of the isotopic labelling regioselectivity under our developed conditions. The computational findings indicated that both complexation events were energetically more favorable than the bis-solvated complex $\mathbf{Int_I}$. Relative to the pyrimidine bound species $\mathbf{Int_{II}^{Py}}$, the sulfoximine conformer $\mathbf{Int_{II}^{S(VI)}}$ was revealed to be energetically more favorable ($\mathbf{Int_{II}^{S(VI)}}$: $-16.0\,kcal\,mol^{-1}$ versus $\mathbf{Int_{II}^{Py}}$: $-14.0\,kcal\,mol^{-1}$), with the same $\mathbf{Int_{II}^{S(VI)}}$ species also possessing a superior binding energy ($-35.4\,kcal\,mol^{-1}$ versus $-33.9\,kcal\,mol^{-1}$ for $\mathbf{Int_{II}^{Py}}$). Following formation of the functional group bound intermediates, the subsequent sulfoximine directed C–H activation transition state was also found to be more facile ($\Delta G\mathbf{TS_I^{S(VI)}}$ $21.0\,kcal\,mol^{-1}$), with the analogous activation of the *ortho*-bond adjacent to the pyrimidine computed to be less susceptible to metallocycle formation ($\Delta G\mathbf{TS_I^{Py}}$ $22.5\,kcal\,mol^{-1}$). These results indicate a dual favorability for the sulfoximine-directed labelling pathway, with the associated potential for BAY1000394 to be selectively labelled in a single step without the requirement for de novo synthesis. Accordingly, we performed the deuterium labelling experiment prior to translation to the more intricate tritiation procedure. As shown in Scheme 3C, a substantial bias was observed for the sulfoximine directed pathway at 50 °C (**[^{2}H]-42**, 91 % D versus 9 % D adjacent to the pyrimidine unit). From this result, we tuned the reaction set up and conditions accordingly, and, in direct alignment with our computational outputs, **42** underwent near-precision tritium labelling adjacent to the sulfoximine unit, delivering a high specific activity of $29.7\,Ci\,mmol^{-1}$ (**[^{3}H]-42**) under sub-atmospheric pressure of T_2 (0.4 atm). Associated with this, it is notable that the prepared radioactive product surpasses the generally accepted requirements for a high specific activity API to possess, at least, an isotopic enrichment of $15\,Ci\,mmol^{-1}$ (0.5 tritiums/molecule).[21]

Following on from this, we extended our substrate scope further whereby the sulfonimidamide analogue of the antihistamine, Loratadine, **43**[32] underwent extremely efficient C–D bond formation in the presence of pyridine and alkene functionalities (97 % D). Collectively, these examples demonstrate the clear applicability of the developed C(sp^2)–H labelling strategy to drug-discovery settings, as well as the synergy between our computational predictive studies and the experimental outcomes.

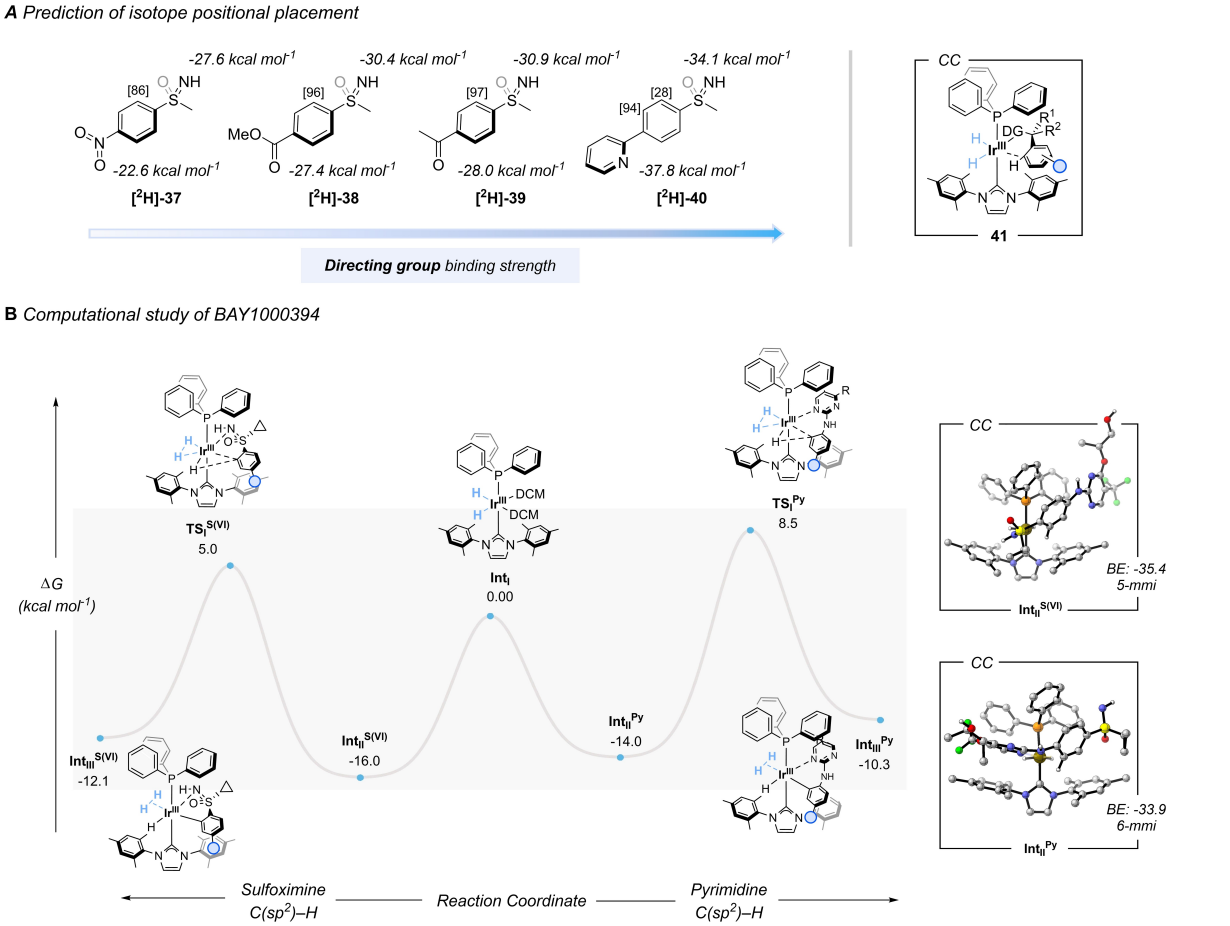

Scheme 3. **A** Prediction of isotope positional placement. Computational studies were utilized for predictions. Experimental results were conducted under standard labelling conditions as described in Scheme 2. **B** Computational study of BAY1000394. Calculation of binding energies, transitions states, and intermediates along the reaction coordinate were used to predict the regioselectivity of the HIE reaction of BAY1000394. **C** Late-stage labelling of pharmaceuticals. Reaction conditions: [a]Pre-catalyst **1** (2.5 mol%), substrate **42** (0.0179 mmol), an atmosphere of deuterium introduced via balloon, EtOAc (0.018 M), 50 °C, 16 h. [b]Pre-catalyst **1** (20 mol%), substrate **42** (1.97 μmol), tritium gas (0.4 atm), 1,2-DCE (0.00328 M), 25 °C, 1 h 40 min. [c]Pre-catalyst **1** (2.5 mol%), substrate **43** (0.0538 mmol), an atmosphere of deuterium introduced via balloon, DCM (0.043 M), 25 °C, 1 h. Binding energies were calculated at the 6-311G(d,p) level of theory.

Although substituted homoarenes are the most prevalent ring system found in pharmaceuticals, featuring in almost 50% of all globally marketed small-molecule drugs,[33] the replacement of this motif with C(sp^3)-hybridized bioisosteres in drug candidates can lead to superior pharmacokinetic properties while retaining biological activity.[34] With this in mind, we set out to develop a labelling strategy for sulfoximine-containing scaffolds that circumvent the requirement for C(sp^2)-character within the immediate vicinity of the directing group. Given the statistical link between the inherent ratio of sp^2 to sp^3 bond content within a given API and clinical success,[35] coupled with the prevalence of *S*-methyl sulfoximine motifs, we recognized the opportunity to exploit our earlier C(sp^3)–H activation mode observations. It was envisaged that the successful development of such a protocol could have appreciable impact in the drug discovery domain, forgoing the need for protracted

synthetic sequences that necessitate the use of hazardous isotopically-labelled alkylating agents. To address this challenge, we hypothesized that complex **1** would act as a basis for the identification of a pre-catalyst more suited to this transformation. Appreciating the difficulty associated with the activation of C(sp^3)–H bonds, we considered the introduction of electron-donating substituents on both the phosphine and *N*-heterocyclic carbene (NHC) components of the catalyst to support C–H activation, whilst maintaining the steric profile of the ligands to drive product formation,[16a,b] an event that can present challenges within iridium catalysis.[36] Using the [Ir(COD)-(P^nBu_3)(IMes)]BAr_F pre-catalyst **44**, a selection of sulfoximine architectures were successfully labelled at the *S*-methyl position, under re-optimized conditions, to provide products with good to excellent enrichments (Scheme 4). Related to this, one-carbon homologation of the sulfoximine functional group from the arene fragment was well-tolerated (**[^{2}H]-45** and **[^{2}H]-46**, 89 % D and 91 % D, respectively), albeit with the fluoro-containing structure **46** still incurring some directed labelling on the aromatic ring. Moreover, the further distancing or complete removal of C(sp^2)-character was shown to be unproblematic (**[^{2}H]-47** and **[^{2}H]-48**, 87 % D and 58 % D, respectively). The increase in steric bulk that results from the replacement of the *S*-methyl with the *S*-ethyl unit in **49** appears to indicate that methylene C(sp^3)–H labelling is more challenging, with multiple labelling pathways now becoming viable. Specifically, the methylene positions adjacent to the sulfoximine as well as the arene ring were now labelling to modest levels. Finally, we performed the late-stage HIE of a protected and sulfoximine-containing derivative of the biomolecule, L–Methionine, **50**, which is completely absent of C(sp^2)-character and where a good 57 % D enrichment was achieved under the standard conditions described in Scheme 4. At this stage, while further studies are on-going, our working hypothesis is that a sterically-driven metalation process delivers selective labelling reactivity preferentially at the *S*-methyl moiety within the substrates investigated.

Conclusions

We have established effective catalytic methods that offer efficient access to highly deuterated and tritiated sulfoximine-containing compounds. Our selection of an appropriate HIE catalyst was guided by the implementation of DFT calculations, specifically investigating individual binding energies within the central coordination complex intermediate. Furthermore, this overall approach has also allowed the prediction and delivery of labelling regioselectivity of arenes within polyfunctionalized molecules and more elaborated pharmaceuticals. Leading on from our *ortho*-directed approach, we have also developed complementary catalytic methods for the introduction of hydrogen isotopes into saturated hydrocarbon frameworks, which permit the expedient synthesis of sulfoximines labelled at C(sp^3)–H sites. The translational synthetic potential of each protocol was further exemplified through the efficient HIE of bioactive molecules and an amino-acid derivative, with the overarching method showing tolerance to the presence of transition-metal-sensitive moieties such as alcohols, amines, esters, halides, heterocycles, and olefins. We anticipate that adoption of these catalytic systems will enable the synthesis of research tools that will accelerate the understanding of

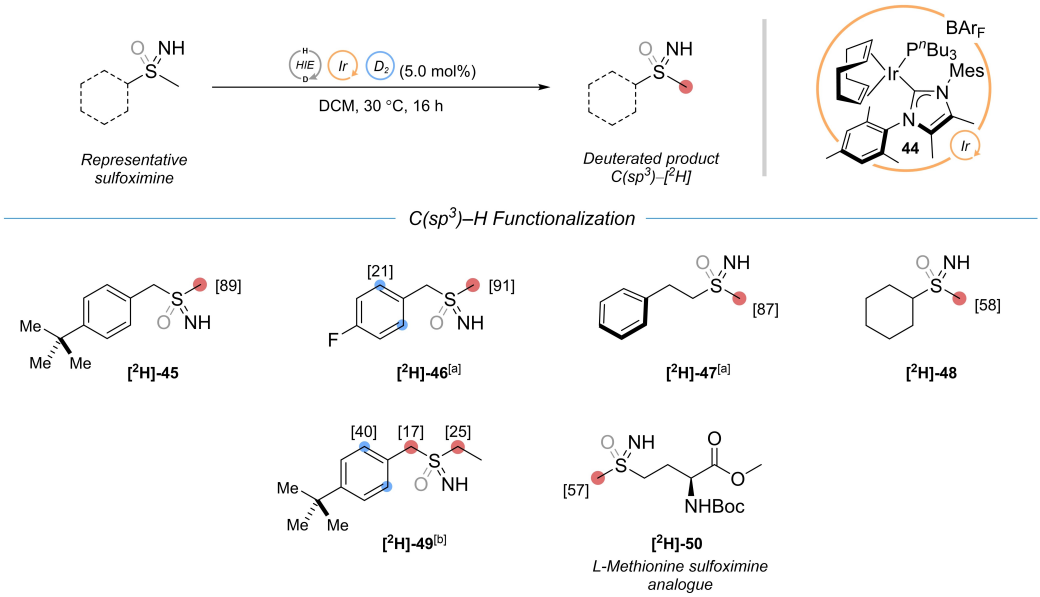

Scheme 4. Evaluation of reaction scope associated with the sulfoximine-directed *S*-alkyl C–H activation sequence. All reactions were performed on a 0.1075 mmol scale with complex **44** (5 mol %) under an atmosphere of deuterium introduced via balloon, in DCM (0.043 M) at 30 °C over 16 h; isotopic incorporation within the isolated products is recorded as an average of, at least, two separate runs. [a]Incorporation was determined from the crude reaction mixture. [b]Reaction was conducted at 40 °C.

the biological performance of drug candidates and, consequently, support the approval of sulfoximine-containing therapeutics.

Supporting Information

The authors have cited additional references within the Supporting Information.[37–77]

Acknowledgements

An EPSRC Industrial CASE PhD Studentship (EP/M507647/1) with additional support from AstraZeneca is gratefully acknowledged. Additionally, the authors thank the University of Strathclyde for PhD studentship funding. We are also grateful to Messrs Liam Raeside and Andrew McAleer, University of Strathclyde, for assistance with data management. We also thank Dr James S. Scott, AstraZeneca, for inspirational discussions prior to the initiation of this study.

Conflict of Interest

The authors declare no conflict of interest.

Data Availability Statement

The data that support the findings of this study are available in the supplementary material of this article.

Keywords: Sulfoximine · Deuterium · Iridium · C–H activation · Hydrogen Isotope Exchange

[1] a) D. C. Blakemore, L. Castro, I. Churcher, D. C. Rees, A. W. Thomas, D. M. Wilson, A. Wood, *Nat. Chem.* **2018**, *10*, 383–394; b) K. R. Campos, P. J. Coleman, J. C. Alvarez, S. D. Dreher, R. M. Garbaccio, N. K. Terrett, R. D. Tillyer, M. D. Truppo, E. R. Parmee, *Science* **2019**, *363*, 1–9; c) J. Boström, D. G. Brown, R. J. Young, G. M. Keserü, *Nat. Rev. Drug Discovery* **2018**, *17*, 709–727.

[2] a) P. Ertl, E. Altmann, J. M. McKenna, *J. Med. Chem.* **2020**, *63*, 8408–8418; b) E. A. Ilardi, E. Vitaku, J. T. Njardarson, *J. Med. Chem.* **2014**, *57*, 2832–2842; c) C. Zhao, K. P. Rakesh, L. Ravidar, W.-Y. Fang, H.-L. Qin, *Eur. J. Med. Chem.* **2019**, *162*, 679–734.

[3] K. A. Scott, J. T. Njardarson, *Top. Curr. Chem.* **2018**, *376*, 1–34.

[4] A. Mullard, *Nat. Rev. Drug Discovery* **2023**, *22*, 83–88.

[5] P. Mäder, L. Kattner, *J. Med. Chem.* **2020**, *63*, 14243–14275.

[6] a) U. Lücking, *Angew. Chem. Int. Ed.* **2013**, *52*, 9399–9408; b) U. Lücking, *Chem. Eur. J.* **2022**, *28*, 1–13; c) U. Lücking, *Org. Chem. Front.* **2019**, *6*, 1319–1324.

[7] a) J. A. Sirvent, U. Lücking, *ChemMedChem.* **2017**, *12*, 487–501; b) M. Frings, C. Bolm, A. Blum, C. Gnamm, *Eur. J. Med. Chem.* **2017**, *126*, 225–245; c) U. Lücking, R. Jautelat, M. Krüger, T. Brumby, P. Lienau, M. Schäfer, H. Briem, J. Schulze, A. Hillisch, A. Reichel, A. M. Wengner, G. Siemeister, *ChemMedChem.* **2013**, *8*, 1067–1085.

[8] a) E. M. Isin, C. S. Elmore, G. N. Nilsson, R. A. Thompson, L. Weidolf, *Chem. Res. Toxicol.* **2012**, *25*, 532–542; b) C. S. Elmore, R. A. Bragg, *Bioorg. Med. Chem. Lett.* **2015**, *25*, 167–171; c) C. S. Elmore, in *Annual Reports in Medicinal Chemistry, Vol. 44* (Ed.: J. E. Macor), Academic Press: Oxford **2009**, pp. 515–534; d) W. J. S. Lockley, A. McEwen, R. Cooke, *J. Labelled Compd. Radiopharm.* **2012**, *55*, 235–257; e) R. Voges, R. Heys, T. Moenius, *Preparation of Compounds Labeled with Tritium and Carbon-14*, Wiley, Chichester, UK **2009**; f) P. H. Allen, M. J. Hickey, L. P. Kingston, D. J. Wilkinson, *J. Labelled Compd. Radiopharm.* **2010**, *53*, 731–738; g) P. Allen, R. A. Bragg, M. Caffrey, C. Ericsson, M. J. Hickey, L. P. Kingston, C. S. Elmore, *J. Labelled Compd. Radiopharm.* **2017**, *60*, 124–129.

[9] J. Atzrodt, V. Derdau, W. J. Kerr, M. Reid, *Angew. Chem. Int. Ed.* **2018**, *57*, 1758–1784.

[10] a) T. Pirali, M. Serafini, S. Cargnin, A. A. Genazzani, *J. Med. Chem.* **2019**, *62*, 5276–5297; b) R. M. C. Di Martino, B. D. Maxwell, T. Pirali, *Nat. Rev. Drug Discovery* **2023**, *22*, 562–584.

[11] J. Atzrodt, V. Derdau, *J. Labelled Compd. Radiopharm.* **2010**, *53*, 674–685.

[12] S. M. Paul, D. S. Mytelka, C. T. Dunwiddie, C. C. Persinger, B. H. Munos, S. R. Lindborg, A. L. Schacht, *Nat. Rev. Drug Discovery* **2010**, *9*, 203–214.

[13] S. Patel, R. Gibson, *Nucl. Med. Biol.* **2008**, *35*, 805–815.

[14] a) J. Atzrodt, V. Derdau, W. J. Kerr, M. Reid, *Angew. Chem. Int. Ed.* **2018**, *57*, 3022–3047; b) S. Kopf, F. Bourriquen, W. Li, H. Neumann, K. Junge, M. Beller, *Chem. Rev.* **2022**, *122*, 6634–6718.

[15] a) R. Salter, *J. Labelled Compd. Radiopharm.* **2010**, *53*, 645–657; b) J. R. Heys, *J. Labelled Compd. Radiopharm.* **2007**, *50*, 770–778.

[16] a) J. A. Brown, S. Irvine, A. R. Kennedy, W. J. Kerr, S. Andersson, G. N. Nilsson, *Chem. Commun.* **2008**, 1115–1117; b) J. A. Brown, A. R. Cochrane, S. Irvine, W. J. Kerr, B. Mondal, J. A. Parkinson, L. C. Paterson, M. Reid, T. Tuttle, S. Andersson, G. N. Nilsson, *Adv. Synth. Catal.* **2014**, *356*, 3551–3562; c) W. J. Kerr, R. J. Mudd, L. C. Paterson, J. A. Brown, *Chem. Eur. J.* **2014**, *20*, 14604–14607; d) G. N. Nilsson, W. J. Kerr, *J. Labelled Compd. Radiopharm.* **2010**, *53*, 662–667; e) W. J. Kerr, G. J. Knox, L. C. Paterson, *J. Labelled Compd. Radiopharm.* **2020**, *63*, 281–295; f) A. R. Cochrane, C. Idziak, W. J. Kerr, B. Mondal, L. C. Paterson, T. Tuttle, S. Andersson, G. N. Nilsson, *Org. Biomol. Chem.* **2014**, *12*, 3598–3603; g) A. R. Kennedy, W. J. Kerr, R. Moir, M. Reid, *Org. Biomol. Chem.* **2014**, *12*, 7927–7931.

[17] J. Devlin, W. J. Kerr, D. M. Lindsay, T. J. D. McCabe, M. Reid, T. Tuttle, *Molecules.* **2015**, *20*, 11676–11698.

[18] a) W. J. Kerr, D. M. Lindsay, P. K. Owens, M. Reid, T. Tuttle, S. Campos, *ACS Catal.* **2017**, *7*, 7182–7186; b) J. Atzrodt, V. Derdau, W. J. Kerr, M. Reid, P. Rojahn, R. Weck, *Tetrahedron.* **2015**, *71*, 1924–1929; c) W. J. Kerr, D. M. Lindsay, M. Reid, J. Atzrodt, V. Derdau, P. Rojahn, R. Weck, *Chem. Commun.* **2016**, *52*, 6669–6672.

[19] P. K. Owens, B. I. P. Smith, S. Campos, D. M. Lindsay, W. J. Kerr, *Synthesis* **2023**, *55*, 3644–3651.

[20] R. P. Yu, D. Hesk, N. Rivera, I. Pelczer, P. J. Chirik, *Nature.* **2016**, *529*, 195–199.

[21] a) Y. Y. Loh, K. Nagao, A. J. Hoover, D. Hesk, N. R. Rivera, S. L. Colletti, I. W. Davies, D. W. C. MacMillan, *Science* **2017**, *358*, 1182–1187; see also b) H. Yang, Z. Huang, D. Lehnherr, Y.-H. Lam, S. Ren, N. A. Strotman, *J. Am. Chem. Soc.* **2022**, *144*, 5010–5022.

[22] a) W. J. Kerr, R. J. Mudd, M. Reid, J. Atzrodt, V. Derdau, *ACS Catal.* **2018**, *8*, 10895–10900; b) N. M. L. Knight, J. D. F.

Thompson, J. A. Parkinson, D. M. Lindsay, T. Tuttle, W. J. Kerr, *Adv. Synth. Catal.* **2024**, *366*, 2577–2586; see also c) M. Valero, R. Weck, S. Güssregen, J. Atzrodt, V. Derdau, *Angew. Chem. Int. Ed.* **2018**, *57*, 8159–8163.
[23] W. J. Kerr, M. Reid, T. Tuttle, *Angew. Chem. Int. Ed.* **2017**, *56*, 7808–7812.
[24] A. Y. L. Shu, W. Chen, J. R. Heys, *J. Organomet. Chem.* **1996**, *524*, 87–93.
[25] a) R. N. Perutz, S. Sabo-Etienne, *Angew. Chem. Int. Ed.* **2007**, *46*, 2578–2592; b) R. N. Perutz, S. Sabo-Etienne, A. S. Weller, *Angew. Chem. Int. Ed.* **2022**, *61*, e202111462.
[26] W. J. Kerr, G. J. Knox, M. Reid, T. Tuttle, J. Bergare, R. A. Bragg, *ACS Catal.* **2020**, *10*, 11120–11126.
[27] W. J. Kerr, M. Reid, T. Tuttle, *ACS Catal.* **2015**, *5*, 402–410.
[28] S. F. Boys, F. Bernardi, *Mol. Phys.* **1970**, *19*, 553–566.
[29] L. Falivene, Z. Cao, A. Petta, L. Serra, A. Poater, R. Oliva, V. Scarano, L. Cavallo, *Nat. Chem.* **2019**, *11*, 872–879.
[30] a) M. Valero, T. Kruissink, J. Blass, R. Weck, S. Güssregen, A. T. Plowright, V. Derdau, *Angew. Chem. Int. Ed.* **2020**, *59*, 5626–5631; for related experimental studies, see b) D. S. Timofeeva, D. M. Lindsay, W. J. Kerr, D. J. Nelson, *Catal. Sci. Technol.* **2020**, *10*, 7249–7255; c) D. S. Timofeeva, D. M. Lindsay, W. J. Kerr, D. J. Nelson, *Catal. Sci. Technol.* **2021**, *11*, 5498–5504.
[31] G. Siemeister, U. Lücking, A. M. Wengner, P. Lienau, W. Steinke, C. Schatz, D. Mumberg, K. Ziegelbauer, *Mol. Cancer Ther.* **2012**, *11*, 2265–2273.
[32] J.-L. Menardo, F. Horak, M. R. Danzig, W. Czarlewski, *Clin. Ther.* **1997**, *19*, 1278–1293.
[33] a) R. D. Taylor, M. MacCoss, A. D. G. Lawson, *J. Med. Chem.* **2014**, *57*, 5845–5859; b) M. A. M. Subbaiah, N. A. Meanwell, *J. Med. Chem.* **2021**, *64*, 14046–14128.
[34] a) A. F. Stepan, C. Subramanyam, I. V. Efremov, J. K. Dutra, T. J. O'Sullivan, K. J. DiRico, W. S. McDonald, A. Won, P. H. Dorff, C. E. Nolan, S. L. Becker, L. R. Pustilnik, D. R. Riddell, G. W. Kauffman, B. L. Kormos, L. Zhang, Y. Lu, S. H. Capetta, M. E. Green, K. Karki, E. Sibley, K. P. Atchison, A. J. Hallgren, C. E. Oborski, A. E. Robshaw, B. Sneed, C. J. O'Donnell, *J. Med. Chem.* **2012**, *55*, 3414–3424; b) Y. P. Auberson, C. Brocklehurst, M. Furegati, T. C. Fessard, G. Koch, A. Decker, L. La Vecchia, E. Briard, *ChemMedChem* **2017**, *12*, 590–598; c) P. K. Mykhailiuk, *Org. Biomol. Chem.* **2019**, *17*, 2839–2849; d) T. A. Reekie, C. M. Williams, L. M. Rendina, M. Kassiou, *J. Med. Chem.* **2019**, *62*, 1078–1095.
[35] a) F. Lovering, J. Bikker, C. Humblet, *J. Med. Chem.* **2009**, *52*, 6752–6756; b) F. Lovering, *Med. Chem. Commun.* **2013**, *4*, 515–519.
[36] K. Shin, Y. Park, M.-H. Baik, S. Chang, *Nat. Chem.* **2018**, *10*, 218–224.
[37] W. L. F. Armarego, C. L. L. Chai, *Purification of Laboratory Chemicals, 7th Edition*, Elsevier Butterworth-Heinemann, Oxford **2013**.
[38] *Gaussian 16, Revision C.01*, M. J. Frisch, G. W. Trucks, H. B. Schlegel, G. E. Scuseria, M. A. Robb, J. R. Cheeseman, G. Scalmani, V. Barone, G. A. Petersson, H. Nakatsuji, X. Li, M. Caricato, A. V. Marenich, J. Bloino, B. G. Janesko, R. Gomperts, B. Mennucci, H. P. Hratchian, J. V. Ortiz, A. F. Izmaylov, J. L. Sonnenberg, D. Williams-Young, F. Ding, F. Lipparini, F. Egidi, J. Goings, B. Peng, A. Petrone, T. Henderson, D. Ranasinghe, V. G. Zakrzewski, J. Gao, N. Rega, G. Zheng, W. Liang, M. Hada, M. Ehara, K. Toyota, R. Fukuda, J. Hasegawa, M. Ishida, T. Nakajima, Y. Honda, O. Kitao, H. Nakai, T. Vreven, K. Throssell, J. A. Montgomery, Jr., J. E. Peralta, F. Ogliaro, M. J. Bearpark, J. J. Heyd, E. N. Brothers, K. N. Kudin, V. N. Staroverov, T. A. Keith, R. Kobayashi, J. Normand, K. Raghavachari, A. P. Rendell, J. C. Burant, S. S. Iyengar, J. Tomasi, M. Cossi, J. M. Millam, M. Klene, C. Adamo, R. Cammi, J. W. Ochterski, R. L. Martin, K. Morokuma, O. Farkas, J. B. Foresman, D. J. Fox, Gaussian, Inc., Wallingford, CT **2016**.
[39] a) Y. Zhao, D. G. Truhlar, *Chem. Phys. Lett.* **2011**, *502*, 1–13; b) A. D. McLean, G. S. Chandler, *J. Chem. Phys.* **1980**, *72*, 5639–5648; c) R. Krishnan, J. S. Binkley, R. Seeger, J. A. Pople, *J. Chem. Phys.* **1980**, *72*, 650–654.
[40] G. Filsak, H. Budzikiewicz, *J. Mass Spectrom.* **1999**, *34*, 601–610.
[41] E. Alwedi, L. N. Zakharov, P. R. Blakemore, *Eur. J. Org. Chem.* **2014**, 6643–6648.
[42] A. Tota, M. Zenzola, S. J. Chawner, S. S. John-Campbell, C. Carlucci, G. Romanazzi, L. Degennaro, J. A. Bull, R. Luisi, *Chem. Commun.* **2017**, *53*, 348–351.
[43] E. L. Briggs, A. Tota, M. Colella, L. Degennaro, R. Luisi, J. A. Bull, *Angew. Chem. Int. Ed.* **2019**, *58*, 14303–14310.
[44] C. M. M. Hendriks, R. A. Bohmann, M. Bohlem, C. Bolm, *Adv. Synth. Catal.* **2014**, *356*, 1847–1852.
[45] S. Gupta, S. Baranwal, N. Muniyappan, S. Sabiah, J. Kandasamy, *Synthesis* **2019**, *51*, 2171–2182.
[46] R. A. Kelly III, H. Clavier, S. Giudice, N. M. Scott, E. D. Stevens, J. Bordner, I. Samardjiev, C. D. Hoff, L. Cavallo, S. P. Nolan, *Organometallics* **2008**, *27*, 202–210.
[47] K. Hirano, S. Urban, C. Wang, F. Glorius, *Org. Lett.* **2009**, *11*, 1019–1022.
[48] W. J. Kerr, R. J. Mudd, J. A. Brown, *Chem. Eur. J.* **2016**, *22*, 4738–4742.
[49] A. M. Haydl, J. F. Hartwig, *Org. Lett.* **2019**, *21*, 1337–1341.
[50] C. P. Zhang, T. Z. Wang, Y. F. Liang, *Chem. Commun.* **2023**, *59*, 14439–14442.
[51] Y. Long, Y. Zheng, R. Shen, B. Xu, X. Zhou, *Sci. Adv.* **2023**, *1002*, 122910–122915.
[52] S. E. Gibson (née Thomas), N. Guillo, A. J. P. White, D. J. Williams, *J. Chem. Soc., Perkin Trans. 1* **1996**, 2575–2581.
[53] A. C. Jones, W. I. Nicholson, H. R. Smallman, D. L. Browne, *Org. Lett.* **2020**, *22*, 7433–7438.
[54] S. Ponra, A. Nyadanu, N. Pan, E. Martinand-Lurin, A. Savy, M. Vitale, L. El Kaim, L. Grimaud, *Org. Process Res. Dev.* **2020**, *24*, 827–834.
[55] E. Boulard, V. Zibulski, L. Oertel, P. Lienau, M. Schäfer, U. Ganzer, U. Lücking, *Chem. Eur. J.* **2020**, *26*, 4378–4388.
[56] F. Takahashi, K. Nogi, H. Yorimitsu, *Eur. J. Org. Chem.* **2020**, 3009–3012.
[57] Y. Uetake, T. Niwa, T. Hosoya, *Org. Lett.* **2016**, *18*, 2758–2761.
[58] S. Dey, S. K. Gadakh, A. Sudalai, *Org. Biomol. Chem.* **2015**, *13*, 10631–10640.
[59] Z.-Y. Li, L. Li, Q.-L. Li, K. Jing, H. Xu, G.-W. Wang, *Chem. Eur. J.* **2017**, *23*, 3285–3290.
[60] N. Barbero, R. Martin, *Org. Lett.* **2012**, *14*, 796–799.
[61] S. K. Kristensen, S. L. R. Laursen, E. Taarning, T. Skrydstrup, *Angew. Chem. Int. Ed.* **2018**, *57*, 13887–13891.
[62] C. D. McCune, M. L. Beio, J. M. Sturdivant, R. de la Salud-Bea, B. M. Darnell, D. B. Berkowitz, *J. Am. Chem. Soc.* **2017**, *139*, 14077–14089.
[63] Z. Zhou, Y. Guo, *Synth. Commun.* **2008**, *38*, 684–696.
[64] A. Lumbroso, V. Coeffard, E. Le Grognec, I. Beaudet, J.-P. Quintard, *Tetrahedron Lett.* **2010**, *51*, 3226–3228.
[65] B. Bhushan, Y. A. Lin, M. Bak, A. Phanumartwiwath, N. Yang, M. K. Bilyard, T. Tanaka, K. L. Hudson, L. Lercher, M. Stegmann, S. Mohammed, B. G. Davis, *J. Am. Chem. Soc.* **2018**, *140*, 14599–14603.
[66] S. C. Davidson, G. d. P. Gomes, L. R. Kuhn, I. V. Alabugin, A. R. Kennedy, N. C. O. Tomkinson, *Tetrahedron* **2021**, *78*, 131784.
[67] M. Zenzola, R. Doran, L. Degennaro, R. Luisi, J. A. Bull, *Angew. Chem. Int. Ed.* **2016**, *55*, 7203–7207.

[68] J. Kim, J. Ok, S. Kim, W. Choi, P. H. Lee, *Org. Lett.* **2014**, *16*, 4602–4605.
[69] G. Zhang, H. Tan, W. Chen, H. C. Shen, Y. Lu, C. Zheng, H. Xu, *ChemSusChem* **2020**, *13*, 922–928.
[70] M. Kahraman, S. Sinishtaj, P. M. Dolan, T. W. Kensler, S. Peleg, U. Saha, S. S. Chuang, G. Bernstein, B. Korczak, G. H. Posner, *J. Med. Chem.* **2004**, *47*, 6854–6863.
[71] F. Izzo, M. Schäfer, R. Stockman, U. Lücking, *Chem. Eur. J.* **2017**, *23*, 15189–15193.
[72] P. M. Matos, W. Lewis, J. C. Moore, R. A. Stockman, *Org. Lett.* **2018**, *20*, 3674–3677.
[73] T. Bach, C. Körber, *Eur. J. Org.* **1999**, 1033–1039.
[74] M. A. Virolleaud, V. Sridharan, D. Mailhol, D. Bonne, C. Bressy, G. Chouraqui, L. Commeiras, Y. Coquerel, J. Rodriguez, *Tetrahedron.* **2009**, *65*, 9756–9764.
[75] V. Pandya, M. Jain, G. Chakrabarti, H. Soni, B. Parmar, B. Chaugule, J. Patel, T. Jarag, J. Joshi, N. Joshi, A. Rath, V. Unadkat, B. Sharma, H. Ajani, J. Kumar, K. V. V. M. Sairam, H. Patel, P. Patel, *Eur. J. Med. Chem.* **2012**, *58*, 136–152.
[76] H. Yu, Z. Li, C. Bolm, *Angew. Chem. Int. Ed.* **2018**, *57*, 324–327.
[77] J. Jover, J. Cirera, *Dalton Trans.* **2019**, *48*, 15036–15048.

Manuscript received: September 6, 2024
Accepted manuscript online: October 30, 2024
Version of record online: November 18, 2024